Explicit Mathematical Formulation and Coverage Consistency of Satellite Constellation Designs for Repeating Ground Track Orbits

Soung Sub Lee*
Department of Aerospace System Engineering, Sejong University, 209, Neungdong-Ro, Gwangjin-Gu, Seoul, 05006, South Korea

***Abstract*- To solve the coverage consistency and launch cost problems of continuous and periodic coverage, this study proposes a regular and symmetric constellation method for repeating ground track orbits and its closed-form solution for constellation design. The equations of motion developed in this study were implemented via a geometric analysis of Ptolemy's deferent and epicycle systems, and the solution was composed of design parameters. Therefore, unlike the existing constellation method, design and analysis can be realized simultaneously and efficiently. The performance of the proposed constellation method was compared with that of a typical Walker constellation in terms of the figure of merit sensitivity and coverage consistency, and its superior performance was verified. In addition, a comparison with Flower constellations using the same repeating ground track orbit was evaluated via launch cost problems and theoretical comparisons with respect to constellation design.**

***Keywords* - repeating ground track orbit; closed-form solution; design parameter; Walker constellation; Flower constellation**

I. INTRODUCTION

Based on a literature survey of satellite constellation methods, the most well-known and common method is to position satellite orbits regularly and symmetrically on a sphere. With respect to Earth observation missions, the two types are broadly classified as kinematically regular and symmetrical distributions of satellite orbits on the Earth's sphere. The first involves the regular deployment of satellite orbits in the space configuration without considering the rotation of the Earth, and the second involves the deployment of satellite orbits considering the rotational characteristics of the Earth.

A representative example of the first case is the well-known Walker constellation. Given that the Walker constellation does not consider Earth's rotation, the angular separation between the satellite and the observation point on the Earth's surface does not significantly influence Earth coverage. The Walker method was developed by Walker and Mozhaev, and thereafter, various studies were conducted based on this method and applied to practical missions [1-9]. The Walker constellation has four design parameters (*i*:t/p/f, where *i* is the inclination of the orbits, t is the total number of satellites, p is the number of orbit planes, and f is the phase parameter) to regularly set inertial circular orbits on the Earth's sphere. Recently, based on these design parameters, research areas have expanded to include improving accuracy and reliability for relative orbit determination of inter-satellite range measurement and analyzing coverage capacity of complex satellite constellations [10, 11].

The second representative constellation method involves the use of a repeating ground-track (RGT) orbit. In this method, the rotation of the Earth directly influences the coverage characteristics. In particular, the altitude of the satellite is a critical factor in calculating the coverage performance. Research using the RGT orbit was extensively conducted in various manners, e.g., on the repeat Sun-Synchronous orbit (RSSO) [12-14], design of the RGT orbit under high-fidelity conditions [15,16], optimization of the RGT orbit [17,18], and target-based RGT design [19,20]. However, the abovementioned studies were focused on improving the coverage performance using the RGT orbit. Moreover, studies were conducted on uniform distributions using repeating space tracks in a given rotating reference system based on Flower constellations (FCs).

Given that the FC was proposed by Mortari and Wilkins (2008), research was conducted on various theories and applications: millimeter-wave radiometers for tropospheric monitoring [21], designs for telecommunications services [22], dual-compatible orbits [23], and two-/three-dimensional (2D/3D) lattice theory

* Professor, Department of Aerospace System Engineering, Sejong University, 209, Neungdong-Ro, Gwangjin-Gu, Seoul, 05006, South Korea; spacein0320@sejong.ac.kr

[24,25]. The original FC has the same relative trajectory with respect to a rotating frame by utilizing the phasing mechanism of the ascending node Ω and the initial mean anomaly M_0 among six orbital elements and six integer parameters ($N_d, N_p, F_d, F_n, F_h, and N_s$). In addition, 2D lattice theory, which is an approach similar to that employed in this study, deviates from the concept of the original FC and is focused on the uniform distribution of satellite orbits such as the Walker constellation, based on different relative orbits.

The abovementioned methods can be classified into continuous and periodic coverage. In the Walker method, the coverage consistency of the satellite, which is the acquisition of consistent images (number of repeated accesses) with the same ground track for the Earth's surface and observation targets in the mission analysis period that forms the RGT orbit in this study, is not considered because the coverage performance is calculated for the stationary Earth sphere. Moreover, FCs have the advantage of coverage consistency, as they provide periodic coverage by orbit compatibility between the Earth and satellites. However, given that different inertial orbits are generally used, launch costs can be high unless the constellation is efficiently designed.

Expanding on the conceptual classification mentioned above, satellite constellation methods have also been studied for a variety of specific purposes: achieving complex regional coverage requirements [26], simple coverage of complex scenarios involving full or partial visibility of a geographic region [27], and satellite constellation design for hurricane monitors [28]. This paper proposes a novel constellation method for the purpose of simultaneously solving the coverage consistency and launch cost problems of continuous and periodic coverage. As an academic contribution, existing constellation methods (Walker, FCs, etc.) require an orbit propagator after constellation design phase; however, the solution in this study consists of design parameters and presents an explicit mathematical formulation that simultaneously performs the design phase that determines the position of the satellite constellation and orbit propagation.

II. RELATIVE ORBIT COMPATIBILITY

The concept of this study starts from the rotation ratio relationship of the satellite orbit to the rotation of a rotating reference frame (e.g., the Earth). To define the notation for this description, the primary orbit (acts as a rotating reference frame) is denoted as *q*-orbit, the secondary orbit is denoted as *p*-orbit, and the two orbits are closed periodic orbits. The angular velocities of each

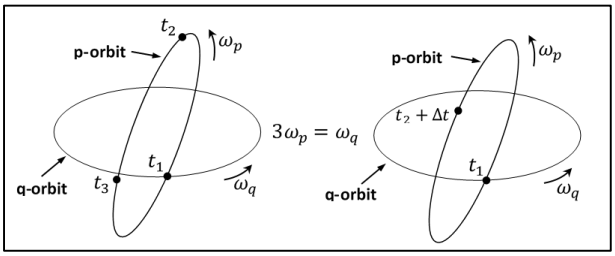

Fig. 1. a) Placement on *p*-orbit with the same relative trajectory with respect to *q*-orbit (*left*), and b) placement on *p*-orbit with the different relative trajectory with respect to *q*-orbit (*right*)

orbit are ω_q and ω_p, respectively, and it is not necessary to have a constant value to apply the proposed method. However, it is assumed that the two orbits have constant angular velocities. Therefore, the periods of each orbit are $T_q = \frac{2\pi}{\omega_q}$ and $T_p = \frac{2\pi}{\omega_p}$, respectively. The *q*-orbit rotates N_q times with angular velocity ω_q, and the *p*-orbit rotates N_p times with angular velocity ω_p. Thus, the relative orbital compatibility of the two orbits is expressed as follows:

$$N_q T_q = N_p T_p \tag{1}$$

An important characteristic of the orbit compatibility in Eq. (1) is that the dynamics of the relative trajectory between the two orbits are continuously repeated and exhibit the same relative trajectory according to the position and distribution of the orbit. Figure 1 presents the characteristics of the relative trajectory according to the orbit compatibility and placement distribution. As shown in Fig. 1 (a), the positions of the three objects, which are the ratios of the number of rotations to the *q*-orbit with respect to the *p*-orbit, are equally spaced:

$$T_j = T_q, \quad (j = 1,2,3) \tag{2}$$

In contrast, as shown in Fig. 1(b), the ratio of the number of rotations with the *q*-orbit with respect to the *p*-orbit to the positions of the two objects, which are different numbers, are equally distributed:

$$T_j + \Delta T = T_q, \quad (j = 1,2) \tag{3}$$

From a comparison of the two relative orbit dynamics, Fig. 1(a) reveals that the three objects in the *p*-orbit have the same relative trajectory with respect to the *q*-orbit. However, the two objects in Fig. 1(b) have different relative trajectories with respect to the *q*-orbit. This is because the objects of the *p*-orbit continuously and repeatedly move with the same pattern at intervals of Period T_q of the *q*-orbit. Consequently, if objects are evenly placed on the secondary orbit by the number of revolutions of the primary orbit, all objects in the secondary orbit have an identical relative trajectory to the

primary orbit. This relationship can be expressed as follows:

$$N_s = N_q \left(\frac{p}{q}\right)_{\perp} \tag{4}$$

where N_s denotes the number of objects. As expressed by Eq. (4), the two positive integers q and p are co-prime, which can be expressed as gcd (p, q) = 1 or $\left(\frac{p}{q}\right)_{\perp}$.

As expressed by Eq. (4), the q-value is a divisor of N_q, the p-value is the number of p-orbits, and the total N_s objects are equally divided by the p-plane to have the same relative trajectory. As an example, if N_q of the primary orbit is set as 100 and N_p of the secondary orbit is set as 1494, 60 objects in the p-orbit have the same relative trajectory as the q-orbit:

$$N_s = 100 \left(\frac{3}{5}\right)_{\perp} \tag{5}$$

Given that p = 3 in Eq. (5), three p-orbit are required, and 20 objects are placed in each plane, where q = 5 is a coprime of the p-value and a divisor of 100.

III. REPEATING GROUND TRACK ORBIT

The previous section presents the orbital compatibility between any rotating gravitational forces of any two orbits. In actual space missions, these characteristics are applied to the RGT orbit between the Earth and satellites. It is common knowledge that the RGT trajectory of a satellite returns to its original position on the Earth's surface by orbit compatibility after a certain interval of the nodal period. From Eq. (1), the following expression is obtained:

$$T_p = \frac{N_q}{N_p} T_q \tag{6}$$

Applying Eq. (6) to the RGT orbit of the Earth and satellite, T_p is the orbit period of the satellite and T_q is the nodal period of the Earth. Thus, N_q and N_p are coprime. In Eq. (6), T_p can be expressed as a function of the semi-major axis a representing the size of the satellite orbit:

$$2\pi \sqrt{\frac{a^3}{\mu}} = \frac{N_q}{N_p} T_q \tag{7}$$

From Eq. (7), the semi-major axis a is expressed as follows:

$$a = \mu^{\frac{1}{3}} \left(\frac{2\pi}{T_q} \frac{N_p}{N_q}\right)^{-\frac{2}{3}} \tag{8}$$

where the gravitational constant μ is $3.98600441 \times 10^{14} (m^3/s^2)$ and the nodal day of Earth T_q is 86164.10035. Equation (8) has constant values, except for N_q and N_p; thus, it can be expressed as follows:

$$h_0 \approx \kappa \left(\frac{N_p}{N_q}\right)^{-\frac{2}{3}} - R_E \tag{9}$$

where the value κ is approximately 42164.173 km and R_E is the Earth's radius.

The altitude obtained from Eq. (9) is clearly an imprecise value that does not consider the effects of orbital perturbations. In practice, calculating the altitude of the RGT orbit by considering the perturbation of the orbit is complex. In this study, only the effect of the J_2 perturbation was considered, and the rotation ratio between the Earth and RGT orbit, which is the relative orbit frequency that defines the altitude of the RGT orbit, is expressed as follows:

$$n + \dot{M} + \dot{\omega} = \frac{N_p}{N_q} (\omega_{\oplus} - \dot{\Omega}) \tag{10}$$

where n, $\dot{M}$, $\dot{\omega}$, $\omega_{\oplus}$, and $\dot{\Omega}$ denote the mean motion of the satellite, change in the mean motion, change in the perigee, rotational velocity of the Earth, and change in the ascending node, respectively. Each element of Eq. (10) under the Earth's J_2 perturbation is defined as follows:

$$\dot{\Omega} = -\frac{3}{2} n J_2 \left(\frac{R_E}{p}\right)^2 cos\, i \tag{11a}$$

$$\dot{\omega} = \frac{1}{2} n J_2 \left(\frac{R_E}{p}\right)^2 (4 - 5\ sin^2 i) \tag{11b}$$

$$\dot{M} = \frac{3}{4} n J_2 \left(\frac{R_E}{p}\right)^2 \sqrt{1 - e^2}\, (3\ cos^2 i - 1) \tag{11c}$$

where $p = a(1 - e^2)$ with the eccentricity e and inclination i of the satellite orbit, the Earth's radius R_E, and J_2 = 0.00108263. Substituting Eq. (10) into Eq. (8), the RGT altitude, considering J_2, is expressed as follows:

$$h = \mu^{\frac{1}{3}} \left[\frac{N_p}{N_q} (\omega_{\oplus} - \dot{\Omega}) - (\dot{M} + \dot{\omega})\right]^{-\frac{2}{3}} - R_E \tag{12}$$

Thus, to obtain the final RGT altitude, the iterative process of Eqs. (9)-(12) is required, and convergence to the final altitude occurs after three to five iterations.

Furthermore, $\frac{N_p}{N_q}$ in Eq. (12) requires a more extensive explanation. A critical factor in designing an RGT orbit is the altitude, which is highly sensitive to the values of N_q and N_p. An effective method to reduce the sensitivity involves the adjustment of the desired altitude via a small change value based on the N_q and N_p values of the reference altitude. The orbit frequency with the simplest ground track structure in the RGT orbit is the case wherein the denominator is 1, which is coprime for all natural numbers. In particular, the altitude of the Earth observation mission, which was of significance in this study, has an orbit frequency range of 14 to 16 and an

altitude of approximately 200 km to 830 km. In addition, $\frac{14}{1}$, $\frac{15}{1}$, and $\frac{16}{1}$, which are fractions with a denominator of 1, are referred to as the principal orbit frequencies. This section presents a method for determining the desired altitude by changing the values of the denominator and numerator based on the principal orbit frequency. The irreducible fraction can be maintained by changing the values of the denominator and numerator of the irreducible fraction $\left(\frac{N_p}{N_q}\right)_\perp$: addition/subtraction and multiplication/division.

Addition/subtraction maintains an irreducible fraction by adding or subtracting another irreducible fraction [29]:

$$\left(\frac{N_p}{N_q}\right)_\perp \pm \left(\frac{p}{q}\right)_\perp = \left(\frac{p'}{q'}\right)_\perp \tag{13}$$

where gcd (N_q, q) = 1. In the multiplication/division method, the irreducible fraction is obtained by multiplying or dividing the irreducible fraction $\left(\frac{N_p}{N_q}\right)_\perp$ by the same value as the denominator N_q:

$$\left(\frac{N_p}{N_q}\right)_\perp \begin{matrix}\times \\ \div\end{matrix} \left(\frac{p}{N_q}\right)_\perp = \left(\frac{p'}{q'}\right)_\perp \tag{14}$$

In a simpler manner, four arithmetic operations are applied to the reference irreducible fraction N_q using 1, which can have all natural numbers as co-primes.

$$\left(\frac{N_p}{N_q}\right)_\perp \pm \left(\frac{1}{q}\right)_\perp = \left(\frac{p'}{q'}\right)_\perp \tag{15}$$

where gcd (N_q, q) = 1. Equation (15) fixes the value of p to 1, and the result has an irreducible fraction regardless of the natural number substituted for the value of q. In particular, as the q value increases, the equation converges to a value close to the principal orbit frequency. Combining these properties with the multiplication /division characteristics of Eq. (14), an irreducible fraction is obtained with faster convergence:

$$\left(\frac{N_p}{N_q}\right)_\perp \pm \left(\frac{1}{q}\right)_\perp \cdot \left(\frac{1}{q}\right)_\perp \cdots = \left(\frac{N_p}{N_q}\right)_\perp \pm \left(\frac{1}{q^m}\right)_\perp \tag{16}$$

for m = 1, 2, 3, ⋯.

Figure 2 presents the results obtained by applying Eq. (16) to the reference principal orbit frequency $\left(\frac{N_p}{N_q}\right)_\perp = \left(\frac{15}{1}\right)_\perp$. As shown in the figure, as the value of q increases, the altitude converges to the reference altitude. In particular, as the value of m increases, the altitude converges rapidly. It should be noted that setting a high q value is advantageous for determining the desired altitude relative to the reference altitude; however, as the numerator of the new irreducible fraction increases, the density of the RGT structure increases.

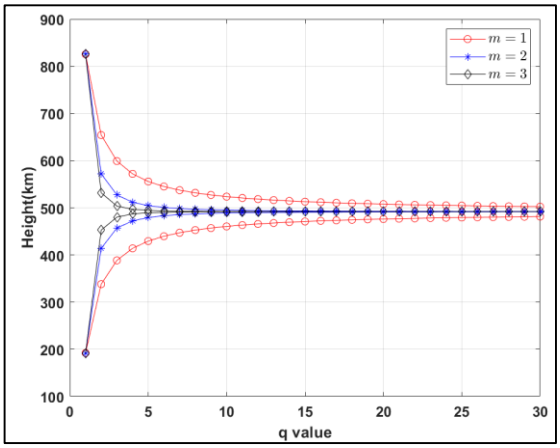

Fig. 2. Convergence to the reference altitude according to the q value

IV. MATHEMATICAL FORMULATION OF RGT CONSTELLATION DESIGN

A. *Geometrical modeling*

As detailed in this section, a closed-form solution of the satellite constellation was developed via geometrical modeling for the RGT design of a circular orbit. For geometrical modeling, Ptolemais' deferent and epicycle systems were employed in this study. Lee and Hall defined that the relative motion of two orbits is determined by the rotation ratio of the two orbits [30]. In particular, if the relative orbit frequency representing the rotation ratio of the two orbits is less than 1, $\left(\frac{N_p}{N_q} < 1\right)$, it is epi-type (epicycloid/epitrochoid) motion, and if it is greater than 1, $\left(\frac{N_p}{N_q} > 1\right)$, it is hypo-type (hypocycloid /hypotrochoid) motion. A representative example of epi-type motion is the orbital motion of the Earth–Moon system, and an example of hypo-type motion is the trajectory between the Earth and a satellite.

The aim of this study was to apply the hypocycloid principle to satellite orbit geometrical mechanics. The RGT geometry on the Earth is the projection of a satellite orbit on a celestial sphere onto the Earth's surface. Thus, considering only the size of the satellite orbit projected on the celestial sphere, as shown in Fig. 3a, it is a function of the semi-major axis a and the inclination i of the satellite. When projected onto the x–y plane of the celestial sphere, the maximum value is a and the minimum value is $a \cos i$, and the trajectory projected on the x–y plane lies between

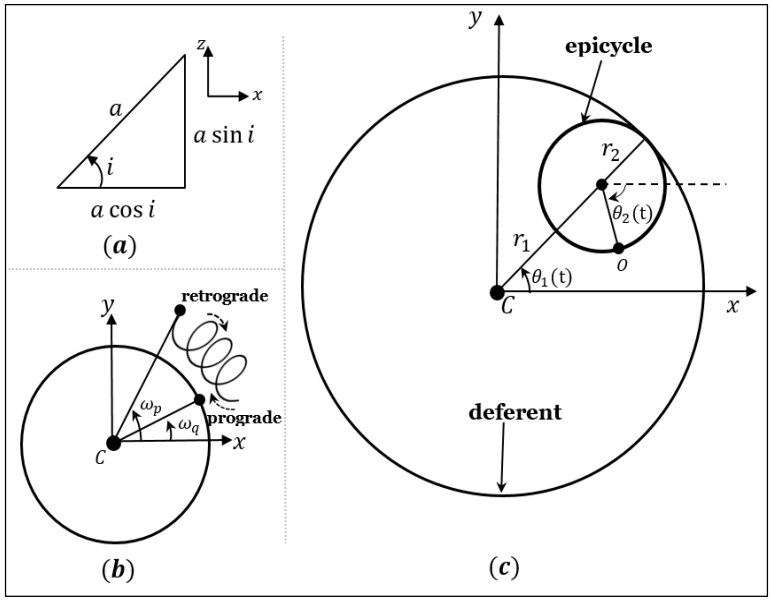

Fig. 3. a) Magnitude of the satellite orbit projected onto the celestial sphere, b) looping motion of satellite orbit, and c) deferent and epicycle system of satellite orbit

these two values. The magnitude of the z-coordinate is $a \sin i$. This determines the size of the circles in deferent and epicycle system. Describing the trajectory properties of the satellite orbit in more detail, the *x*–*y* plane is represented by the relationship between the angular rate ω_q of the rotating reference frame of the Earth and the angular rate ω_p of the satellite, as shown in Fig. 3b. It should be highlighted that the trajectory of the satellite orbit traces a looping motion, as shown in Fig. 3b, which is caused by the prograde and retrograde motions respectively generated by the sum and difference of the two angular rates. This looping motion is observed as loops or cusps (i.e., sharp corners) on the trajectory depending on the inclination of the satellite. If the geometric characteristics of this satellite orbit trajectory are expressed in a hypocycloid geometry on the *x*–*y* plane, it shows the hypocycloid geometry of the deferent and epicycle system as shown in Fig. 3c. The *z*-axis motion is in accordance with a simple spring-mass system. Thus, the parametric formula of the satellite orbit is expressed in a generalized hypocycloid form as follows [31]:

$$x = r_1 \cos\theta_1(t) + r_2 \cos\theta_2(t) \tag{17a}$$

$$y = r_1 \sin\theta_1(t) - r_2 \sin\theta_2(t) \tag{17b}$$

$$z = r_3 \sin\theta_3(t) \tag{17c}$$

As detailed in this section, each term in Eq. (17) can be obtained via a geometric analysis. As shown in Fig. 3c, the radii of the large and small epicycle circles are obtained as follows:

$$r_1 + r_2 = a \tag{18a}$$

$$r_1 - r_2 = a \cos i \tag{18b}$$

From Eq. (18), r_1 and r_2 are respectively expressed as follows:

$$r_1 = \frac{a}{2}(1 + \cos i) \tag{19a}$$

$$r_2 = \frac{a}{2}(1 - \cos i) \tag{19b}$$

As shown in Fig. 3c, the angular rate $\theta_1(t)$ of the deferent circle is related to the prograde motion of the satellite orbit and can be obtained as the difference between the Earth's angular rate and that of the satellite:

$$\theta_1(t) = (\omega_p - \omega_q)t + \theta_{10} \tag{20}$$

where θ_{10} is the initial angular position of deferent circle. The angular rate $\theta_2(t)$ of the epicycle circle is a retrograde motion, which is expressed as follows:

$$\theta_2(t) = (\omega_p + \omega_q)t + \theta_{20} \tag{21}$$

where θ_{20} denotes the initial angular position of the circle. Thereafter, the magnitude and angular rate of the satellite orbit along the *z*-axis can be simply expressed as follows:

$$r_3 = a \sin i \tag{22a}$$

$$\theta_3(t) = \omega_p t + \theta_{30} \tag{22b}$$

To represent Eqs. (18)–(22) with the well-known six orbit elements considering the J_2 perturbation, the parameters ω_p and ω_q are defined as follows:

$$\omega_p = n + \dot{M} + \dot{\omega} \tag{23a}$$

$$\omega_q = \omega_{\oplus} - \dot{\Omega} \tag{23b}$$

In addition, the initial phase angles θ_{10}, θ_{20}, and θ_{30} of the deferent and epicycle circles are expressed as functions of the initial mean anomaly M_0 and ascending node Ω by applying the principles of prograde and retrograde motion:

$$\theta_{10} = M_0 + \Omega, \quad \theta_{20} = M_0 - \Omega, \quad \theta_{30} = M_0 \tag{24}$$

Therefore, by substituting the orbit parameters of Eqs. (18)-(24) into Eq. (17), the equations of motion for the RGT orbit on the Earth can be obtained.

B. Closed-form solution

The aim of this study was to develop a closed-form solution for the design of an RGT constellation as a parameter term for orbit compatibility. As a result of the study, RGT orbit-based constellations were designed with four constellation design parameters: inclination i, total number of satellites N_s, and orbit compatibility N_q and N_p. The satellite group was arranged in accordance with the Walker-type configuration. However, the difference was that the satellite constellation had the same orbital plane and relative trajectory. For a constellation to have the same orbital plane, satellites are equally spaced in the Earth-Centered Inertial (ECI) coordinate frame. Moreover, the constellation of satellites with the same relative trajectory in the Earth-Centered Earth-Fixed (ECEF) coordinate frame is implemented by the phasing mechanism of (Ω, M_0) [32]:

$$\Omega_k = \Theta_{\Omega}(k-1) \tag{25a}$$

$$M_{k0} = -\frac{N_p}{N_q}(k-1) \tag{25b}$$

where k = 1, 2, 3, $\cdots, N_s$, and Θ_{Ω} is the spacing of ascending nodes between satellites. Equation (25) is expressed as follows to distribute N_s constellations at equal intervals:

$$\Omega_k = \frac{2\pi}{N_s} N_q (k-1) \tag{26a}$$

$$M_{k0} = -\frac{2\pi}{N_s} N_p (k-1) \tag{26b}$$

where k = 1, 2, 3,$\cdots, N_s$. Using Eqs. (1), (10), and (23) to express the relative orbit compatibility of the RGT orbit, the following relationship is obtained:

$$N_q T_q = N_q \frac{2\pi}{\omega_q} = N_p T_p = N_p \frac{2\pi}{\omega_p} \tag{27}$$

From Eq. (27), the following is obtained:

$$\omega_q = \frac{2\pi}{T_q}, \qquad \omega_p = \frac{2\pi}{T_p} \tag{28}$$

Moreover,

$$T_q = \frac{N_p}{N_q} = T_p \tag{29}$$

Thus, Eq. (20) can be expressed using Eqs. (24), (26), (28), and (29):

$$\theta_1(t) = (\omega_p - \omega_q)t + \theta_{10} \tag{30a}$$

$$= 2\pi\left(\frac{1}{T_p} - \frac{N_q}{N_p T_p}\right)t - 2\pi\left(\frac{N_p - N_q}{N_s}\right)(k-1) \tag{30b}$$

$$= \left(\frac{N_p - N_q}{N_p}\right)\tau - 2\pi\left(\frac{N_p - N_q}{N_s}\right)(k-1) \tag{30c}$$

where $\tau = 2\pi\frac{t}{T_p}$. Similarly, Eq. (21) is represented by Eqs. (24), (26), (28), and (29).

$$\theta_2(t) = \left(\frac{N_p + N_q}{N_p}\right)\tau - 2\pi\left(\frac{N_p + N_q}{N_s}\right)(k-1) \tag{31}$$

Thereafter, $\theta_3(t)$ of Eq. (22) is expressed as follows:

$$\theta_3(t) = \tau - 2\pi\left(\frac{N_p}{N_s}\right)(k-1) \tag{32}$$

Finally, Eq. (17) represents a completely closed-form solution for the RGT constellation design of N_s satellite group in terms of only four constellation design parameters ($i, N_s, N_p,$ and N_q) while acting as an orbit propagator.

$$\begin{aligned} x_k = {} & A\cos\left[\left(\frac{N_p - N_q}{N_p}\right)\tau - 2\pi\left(\frac{N_p - N_q}{N_s}\right)(k-1)\right] \\ & + B\cos\left[\left(\frac{N_p + N_q}{N_p}\right)\tau - 2\pi\left(\frac{N_p + N_q}{N_s}\right)(k-1)\right] \end{aligned} \tag{33a}$$

$$\begin{aligned} y_k = {} & A\sin\left[\left(\frac{N_p - N_q}{N_p}\right)\tau - 2\pi\left(\frac{N_p - N_q}{N_s}\right)(k-1)\right] \\ & - B\sin\left[\left(\frac{N_p + N_q}{N_p}\right)\tau - 2\pi\left(\frac{N_p + N_q}{N_s}\right)(k-1)\right] \end{aligned} \tag{33b}$$

$$z_k = C\sin\left[\tau - 2\pi\left(\frac{N_p}{N_s}\right)(k-1)\right] \tag{33c}$$

where

$$A = \frac{\kappa}{2}\left(\frac{N_p}{N_q}\right)^{-\frac{2}{3}}(1 + \cos i) \tag{34a}$$

$$B = \frac{\kappa}{2}\left(\frac{N_p}{N_q}\right)^{-\frac{2}{3}}(1 - \cos i) \tag{34b}$$

$$C = \kappa\left(\frac{N_p}{N_q}\right)^{-\frac{2}{3}}\sin i \tag{34c}$$

In addition, the closed-form solutions of Eqs. (33) and (34) are applied to the sun-synchronous orbit, and given that the $\cos i$ term is constant, the four design parameters are reduced to three parameters ($N_s, N_p,$ and N_q). The $\cos i$ term is expressed as a function of the semi-major axis a.

$$cos\, i = -\left(\frac{a}{12352}\right)^{\frac{7}{2}} \tag{35}$$

Equation (35) is obtained by setting the semi-major axis a in Eq. (8) constant as follows:

$$cos\, i = -73.4890\left(\frac{N_p}{N_q}\right)^{-\frac{7}{3}} \tag{36}$$

Therefore, when Eq. (36) is substituted in the $\cos i$ term of Eq. (34), the RGT constellation of the sun-synchronous orbit is designed with only three design parameters.

Equations (33) and (34) clearly express the design of a kinematically regular RGT constellation without computational effort, and with only four design parameters. Compared with the well-known Walker constellation, the solution in this study is composed of terms related to orbit compatibility and the number of satellites, and because it defines the RGT altitude and orbital plane, the RGT constellation is designed like a Walker constellation without an orbit propagator. In this paper, the solutions to Eqs. (33) and (34) are referred to as the RGT-Walker (RGT-W) constellation for comparison with other satellite constellation techniques. The RGT-W closed-form solution of Eqs. (33) and (34) provides several implications for constellation design. First, the equations itself consists of the terms of rotation ratio $\left(\frac{N_p}{N_q}\right)$ of the Earth and satellite; thus, it is possible to directly design the constellation without considering the effects of perturbation such as J_2 oblateness. The problem of satellite constellation design and perturbation effect can be analyzed independently. In addition, Eqs. (33) and (34) are composed of variables such as the mission analysis time t of the RGT orbit and number of satellites k if the design parameters are constant. Therefore, the mission designer expresses a specific constellation as a simple parametric equation consisting of t and k terms. For example, the parametric equation of the RGT-W constellation for 8 satellites with $N_q = 2$, $N_p = 29$ and an inclination 43° is expressed as follows:

$$\begin{aligned} x_k = {} & 6091.8\, cos[0.000996t - 21.47(k-1)] \\ & + 945.23\, cos[0.0011t \\ & - 24.61(k-1)] \end{aligned} \tag{37a}$$

$$\begin{aligned} y_k = {} & 6091.8\, sin[0.000996t - 21.47(k-1)] \\ & - 945.23\, sin[0.0011t \\ & - 24.61(k-1)] \end{aligned} \tag{37b}$$

$$z_k = 4799.2\, sin[0.001t - 24.04(k-1)] \tag{37c}$$

The above advantages of RGT-W reduce the significant computational load for mission designers and help to analyze various characteristics of a particular satellite constellation.

V. THE RGT-W CONSTELLATION DESIGN

As detailed in this section, various constellations were designed based on the solution proposed in the previous section. The characteristics of the RGT-W constellation are as follows: the satellite group is uniformly and regularly distributed in the ECI frame, which is similar to the Walker method, and has an identical RGT in the ECEF frame. The notations and common characteristics of the constellation design are as follows:

(1) $\chi_p^{N_s} = i : N_s, N_p, N_q,$

- $\chi_p^{N_s}$: total number of satellites N_s in p orbital planes
- i: inclination of satellite group
- N_p: number of satellite orbit revolutions to form RGT
- N_q: number of Earth rotations to form an RGT

where $N_s = N_q \left(\frac{p}{q}\right)_{\perp}$.

(2) All satellites are in circular orbits with the same inclination and altitude.

Based on the characteristics above, the RGT-W constellation exhibits three broad types of patterns: a sequential constellation, simultaneous constellation, and sun-synchronous constellation. Figure 4a presents the sequential pattern of χ_2^{48}=45°:48,61,24 with an altitude of 16,260 km, and there are 48 satellites with 24 satellites in one orbital plane. As shown in Fig. 4a, the ECI frame has two orbital planes, and the constellation pattern on the Earth's surface has two inclined circular shapes. This circular pattern involves two kinematic behaviors: 1) the distance between satellites on the circular pattern is maintained and 2) the satellite group passes sequentially over the target area. Additionally, based on the same latitude, the time interval between sequentially moving satellites is calculated from the orbit compatibility:

$$P_t = \frac{86400 \cdot 3600 \cdot N_q}{N_p \cdot N_s}\ (sec) \tag{38}$$

Figure 4b presents the simultaneous pattern of $\chi_{16}^{48} = 45°: 48, 16, 3$. The altitude of the satellite group is 7425.7 km, and there are 48 satellites in 16 orbital planes with three satellites per orbital plane. In Fig. 4b, three horizontal circular patterns can be observed, and these constellation patterns are accompanied by the following dynamic characteristics: 1) The satellite spacing on the circular pattern is largest at the equator and narrowed toward the poles. In particular, the phenomenon of the gathering and moving away of the satellite group is repeated. 2) The satellite group passes simultaneously over the same latitude. The sequential constellation is designed using the following relational expression:

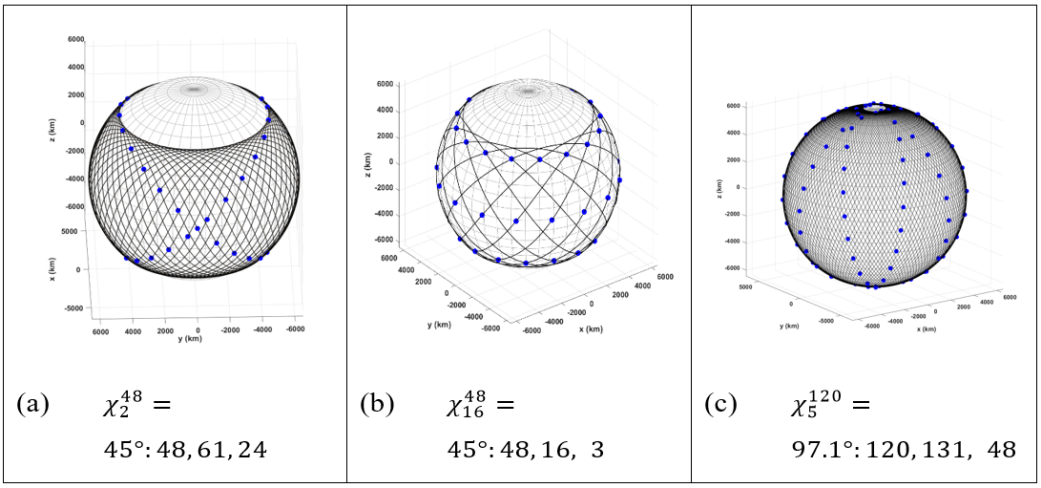

Fig. 4. a) Sequential constellation, b) simultaneous constellation, and c) sun-synchronous constellation

$$N_q \cdot N_p = N_s \tag{39}$$

Figure 4c presents the sun-synchronous constellation of $\chi_5^{120} = 97.1°: 120, 131, 48$ with an altitude of 15211 km and 120 satellites deployed in five orbital planes.

Figure 5 presents the (Ω, M_0) values for the three constellation designs. The value Ω on the *x*-axis indicates an orbital plane in the ECI frame for constellation, and it can be seen that satellites are uniformly distributed in each orbital plane.

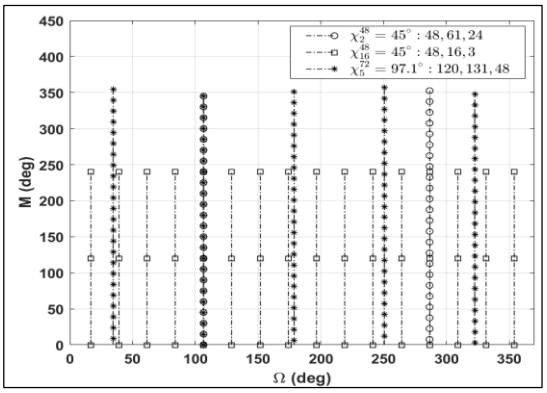

Fig. 5. $(\boldsymbol{\Omega}, \boldsymbol{M_0})$ phasing mechanism of RGT-W constellation

VI. RESULTS AND DISCUSSION

The proposed RGT-W constellation technique can be used to perform preliminary mission design and analysis while minimizing the computational effort without an orbit propagator via a closed-form solution consisting of only three to four design parameters. This section presents the validation of the proposed method via a performance comparison analysis between the proposed RGT-W technique and the prominent Walker constellations and FCs. The RGT-W technique was compared with the conventional Walker technique with respect to coverage consistency and with FC in terms of reducing the orbital plane.

A. Coverage consistency analysis

In this section, to examine the characteristics of the coverage consistency of the proposed RGT-W method, we analyzed the accessibility of random ground targets. The position vector $\vec{r}(x, y, z)$ of the satellite required to calculate the number of RGT orbit accesses to the target is readily obtained by Eqs. (33) and (34), and based on this, the SSP (Sub-Satellite Point, $\alpha_s: Longitude$, $\delta_s: Latitude$) of the ground track on the Earth's surface is as follows:

$$\alpha_s = tan^{-1}\left(\frac{y}{x}\right) \tag{40a}$$

$$\delta_s = sin^{-1}\frac{z}{a} \tag{40b}$$

The accessibility to the target is determined by whether the Earth central angle (Θ) is included in the range of the given sensor swath of the satellite, and the Earth central angle between the target and SSP is obtained by

$$\Theta = cos^{-1}[cos\,\delta_s(t)\,cos\,\delta\,cos(\alpha_s(t) - \alpha) + sin\,\delta_s(t)\,sin\,\delta] \tag{41}$$

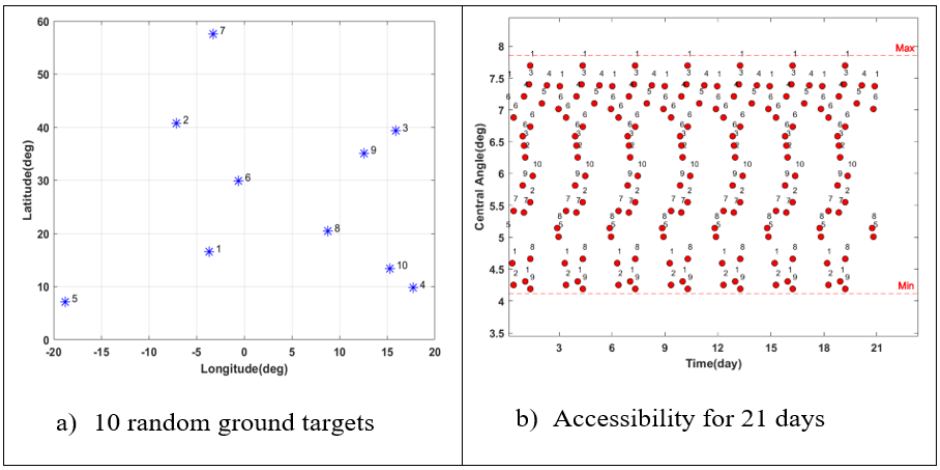

Fig. 6. Accessibility analysis for 10 random ground targets

where α and δ are the longitude and latitude of the target, respectively.

The priority factor to be considered for the coverage consistency analysis of RGT-W is the mission analysis period. The mission analysis period of the RGT orbit is given by N_q, and the ground track is periodically repeated by the value of N_q. Using Eq. (16), a RGT orbit with a mission analysis period of 3 days is selected from the reference principal orbit frequency $\left(\frac{15}{1}\right)_{\perp}$:

$$\left(\frac{15}{1}\right)_{\perp} \pm \left(\frac{1}{3^m}\right)_{\perp} = \left(\frac{44}{3}\right)_{\perp} \tag{42}$$

where m=1; thus, the altitude of $\left(\frac{44}{3}\right)_{\perp}$ is 597.7 km. As shown in Fig. 6a, the ground target was randomly set between longitude $(\pm 20°)$, latitude$(0\sim60°)$, and Table 1 shows the SAR payload and orbital specifications of the satellite.

TABLE I. SATELLITE ORBIT AND SAR PAYLOAD SPECIFICATIONS

N_p/N_q	$i(°)$	$\Omega(°)$	$M_0(°)$	Elevation angle(°)
44/3	61.58	-11.9	31.1	30~50

Figure 6b shows the access results for 10 ground targets for a total of 21 days using the satellite specifications in Table 1. It can be clearly observed that the target accessibility has a repetitive and identical access pattern with a mission analysis period of 3 days.

B. The RGT-W in comparison with the Walker constellation

The existing conventional Walker method achieves global coverage through equally spaced distribution of satellite orbits on the Earth sphere. The Walker method does not include the definition of altitude setting on the satellite phasing rule (*i*: t/p/f): *i* is the inclination, t is the total number of satellites, p is the number of equally spaced planes, and f is the relative spacing between satellites in adjacent planes. Thus, in general, mission designers allow drift of the ground track from the viewpoint of any observed target in the case of Walker method. On the contrary, in the RGT-W method proposed in this study, the definition of altitude and the satellite phasing rule for equally spaced distribution of satellite groups are implicitly included in the formula itself.

To prove the clear difference between the two methods, the constellations are arranged under the same conditions for 24 satellites using the RGT-W and Walker methods. The constellation of Table 2 has 8 evenly spaced orbital planes on the equator, and 3 satellites are arranged on each orbital plane. Orbital elements such as altitude and inclination of the constellation are identical, with the only difference being the initial mean anomaly on the orbital plane. With this difference, the constellation of Walker method has 8 orbital planes and 8 RGT orbits, and RGT-W has 8 orbital planes and 1 RGT orbit. As shown in Fig. 7, the difference between the two methods greatly affects the coverage consistency. Figure 7a shows the ascending node (Ω) and initial mean anomaly (M_0) distributions of 24 satellites, and the distribution of ascending node of the two methods is the same; however, the distribution of initial mean anomaly is different. Figure 7b shows the elevation angle of the satellite sensor during the 3-day mission analysis period for one arbitrary ground target (127.978°, 37.5665°). In the case of RGT-W, only 3 elevation angles are required during the 3-days mission analysis period, whereas the Walker method changes to various elevation angles according to access. This

TABLE II. SPECIFICATIONS FOR COMPARISON BETWEEN THE RGT-W AND WALKER METHODS

RGT-W (χ_3^{24}: 43°, 44, 3)				Walker(43°: 24, 8, 1)			
i(°)	N_s	N_p	N_q	i	t (total)	p (plane)	f
43	24	44	3	43	24	8	1

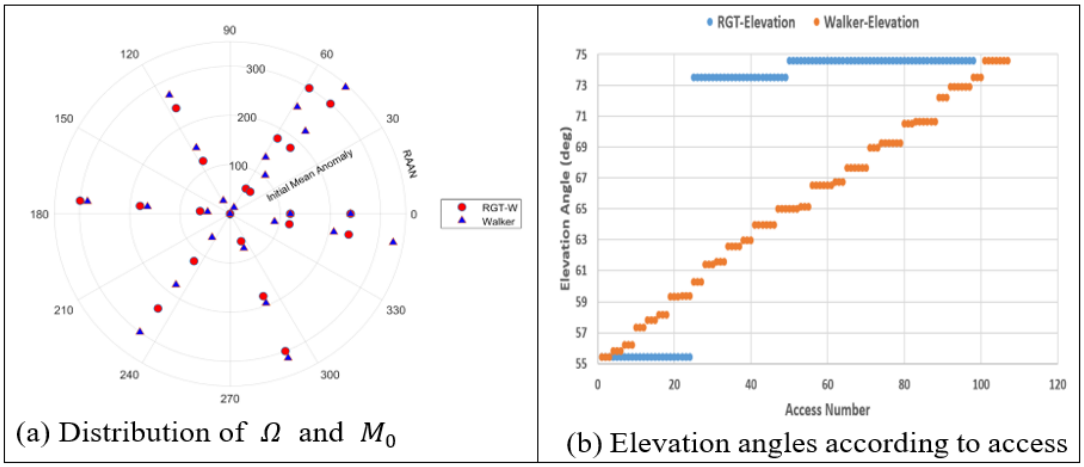

Fig. 7. Comparison of coverage consistency between RGT-W and Walker methods

characteristic is continuously repeated at 3-days intervals throughout the entire mission. Thus, RGT-W has a clear superiority in consistent target observation compared to the Walker method.

Next, for comparison of coverage consistency according to altitude, the FOMs (Figure of Merits) sensitivity of the two techniques were compared with respect to the average revisit time (ART) and system response time (SRT). The ART refers to the time required to re-observe the same observation area, and the SRT is the time elapsed from the capturing of a satellite image to its distribution upon the arrival of an image request for an unplanned area. A critical factor for the comparison of the ART and SRT between the two techniques is the selection of the altitude, which characterizes the RGT and non-RGT orbits. As expressed by Eq. (4), the altitude of the RGT-W technique is determined by the number of satellites and orbital planes. However, the satellite altitude of the Walker technique is a free parameter, which is different from the altitude calculated using Eq. (12). The altitude of the Walker techniques in this study was the integer altitude obtained by truncating the decimal point from the RGT altitude, which ranged from tens to hundreds of meters from the RGT altitude and did not have a significant effect on the FOM performance comparisons between the two techniques,

The similarity observed between the RGT-W and Walker techniques was that the satellite group was

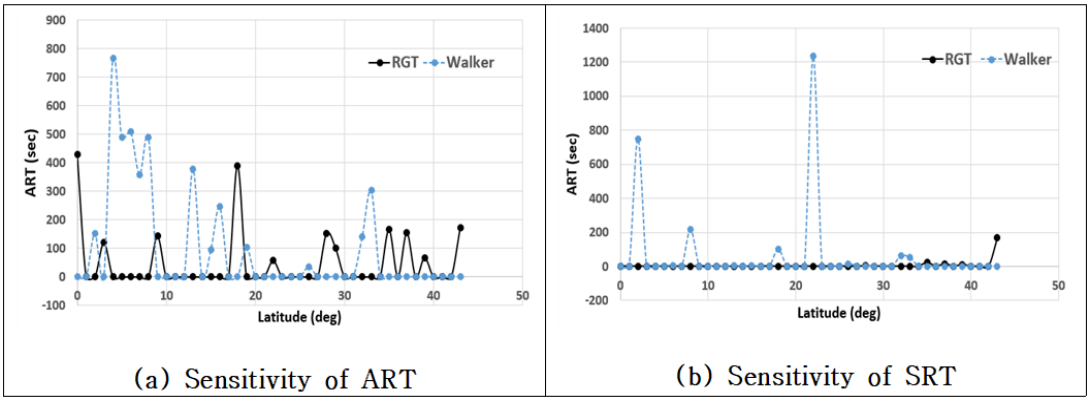

Fig. 8. Sensitivities of ART and SRT with respect to both techniques

uniformly distributed on a unit sphere and exhibited symmetrical characteristics. These symmetrical properties have more longitudinal effects than horizontal effects. For the sensitivity analysis of the FOM, one target was positioned for a specific RGT orbit while changing the latitude from 0° to 43° at intervals of 1° on the same longitude, and the relative differences of the ART and SRT between the two techniques were analyzed. Figure 8 presents the relative difference in values by latitude between RGT-W ($\chi_2^{36} = 43°: 36, 269, 18$) of 508.084 km and Walker ($43°: 36/2/1$) of 508 km. The mission analysis period was 18 days, which is the repeat cycle of the RGT-W. As shown in Fig. 8a, the ART generally maintained the relative values of the RGT-W and Walker techniques within a range of 0 s to 400 s; however, in the case of the Walker technique, the difference in relative values when compared with the RGT-W technique was large at low-latitude targets. In the SRT shown in Fig. 8b, the relative value of the Walker technique changed abruptly at a specific latitude when compared with that of the RGT-W technique. This was evaluated based on the influence of the coverage consistency of the satellite. More specifically, the characteristics of the ground track on the Earth's surface are that the upper part of the trajectory is dense, while the lower part (towards the equator) is wide; thus, the drift in the ground track of the Walker altitude is relatively large compared to the RGT trajectory.

C. The RGT-W in comparison with the Flower constellation

A representative constellation technique using an RGT orbit is the FC. This technique was proposed by Mortari and Wilkins (2008) [22], and the original FC was designed such that all satellites had the same relative trajectory for a rotating reference frame. The disadvantage of the original FC is its high launch cost, given that each satellite is required to have a different ascending node Ω for the same relative trajectory:

$$\Omega_{k+1} = \Omega_k - 2\pi \frac{F_n}{F_d} \tag{43}$$

where F_n and F_d are independent integer parameters that can be freely chosen. The method further developed based on the original FC is the Lattice theory proposed by Avendño and Mortari (2013) [24, 25]. This objective of this theory is to distribute the satellites evenly via distinct relative trajectories in the constellation configuration space, which deviates from the original FC concept, wherein all satellites have the same relative trajectory.

The RGT-W technique was designed such that the satellite group is in the same orbital plane in the ECI frame and has the same relative trajectory at the same time. In Lattice theory, the condition for the satellite constellation to satisfy this objective is mentioned

$$N_q = \lambda N_{so}, \;\; N_p = \mu N_o + \lambda N_c \tag{44}$$

where N_{so} is the number of satellites per orbital plane, and N_o is the number of orbital planes. Moreover, λ and μ are two coprime integers, and $N_c \in [1, N_o]$. In this section, to demonstrate a clear difference between the RGT-W technique and Lattice theory, it is mathematically proven that the simultaneous constellation design of RGT-W cannot be achieved based on Eq. (44). The condition for the simultaneous constellation design in Eq. (39) is expressed as follows:

$$N_q N_p = N_o N_{so} = N_s \tag{45}$$

Substituting Eq. (44) into Eq. (45) yields the following:

$$N_o N_{so} = \lambda N_{so}(\mu N_o + \lambda N_c) \tag{46}$$

This can be re-written as follows:

$$N_c \lambda^2 = N_o(1 - \lambda\mu) \tag{47}$$

Given that $N_c \geq 1$ in lattice theory, $1 - \lambda\mu > 1$ should be satisfied. However, this cannot be achieved. Additionally, Eq. (47) is expressed in a quadratic form in terms of λ.

$$N_c \lambda^2 + \mu N_o \lambda - N_o = 0 \tag{48}$$

The solution to Eq. (48) is expressed as follows:

$$\lambda = \frac{-\mu N_o \pm \sqrt{(\mu N_o)^2 + 4 N_c N_o}}{2 N_c} \tag{49}$$

For the RGT-W technique, $\lambda = 1$ is required; however, Eq. (49) cannot have an integer of $\lambda = 1$. Therefore, Eq. (44) cannot be used to design the simultaneous constellation of the RGT-W technique.

In summary, the RGT-W technique demonstrated a superior performance to the Walker technique in terms of the FOM sensitivity and coverage consistency. Compared with the original FC that uses the RGT orbit, the RGT-W technique can be implemented to design the same relative trajectory while minimizing the orbital plane and launch cost.

VII. CONCLUSIONS

In general, implementing analytical formulas for the constellation designs of multiple satellites is extremely complex. This is because the analytical formula should incorporate the role of the orbit propagator and design parameters. Thus, most previous studies on constellation methods were focused on either design parameters or orbit propagators, and used either classical two-body system or orbit propagators. In contrast to previous studies centered on constellation design parameters, this study focused on the development of an analytical formula based on the equations of motion for

constellation designs. To this end, the equations of motion of the RGT orbit were derived using a geometric model, and a complete closed-form solution consisting of constellation design parameter terms was developed by combining it with orbit compatibility.

This study presents three constellation types based on the solution, and the proposed constellation method is superior to the Walker constellation technique in terms of the FOM sensitivity and coverage consistency. Moreover, it minimizes the launch cost when compared to the original FC using the same RGT orbit.

ACKNOWLEDGEMENT

The Ministry of National Defense of the Republic of Korea is planning to invest more than 1 trillion won to develop a micro-satellite system project equipped with SAR in order to strengthen surveillance and reconnaissance capabilities in areas of interest in Northeast Asia. This study has no direct relevance to this project and does not include military security content.

FUNDING

This work was supported by a grant-in-aid of IITP.

REFERENCES

[1] J.G. Walker, Circular orbit patterns providing continuous whole earth coverage, Royal Aircraft Establishment Technical Report 70211, 1970.

[2] J.G. Walker, Some circular orbit patterns providing continuous whole earth coverage, J. Br. Interplanet. Soc. 24 (1971) 369–384.

[3] J.G. Walker, Continuous whole earth coverage by circular orbit satellite patterns, Royal Aircraft Establishment Technical Report 77044, 1977.

[4] J.G. Walker, Satellite patterns for continuous multiple whole-earth coverage, Maritime and Aeronautical Satellite Communication and Navigation, IEEE Conf. Publ. 160 (1978) 119–122.

[5] G.V. Mozhaev, The problem of continuous earth coverage and kinematically regular satellite networks, I, Kosmicheskie Issledovaniya (Cosmic Res.). 10 (1972) 833–840.

[6] G.V. Mozhaev, The problem of continuous earth coverage and kinematically regular satellite networks, II," *Kosmicheskie Issledovaniya*. 59–69. Translated in *Cosmic Res*, 11, 1 (1973) 11, l 52–61.

[7] T.J. Lang, Symmetric circular orbit satellite constellations for continuous global coverage, in: AAS/AIAA Astrodynamics Specialist Conference, Kalispell, Montana, 1987.

[8] T.J. Lang, W.S. Adams, A comparison of satellite constellations for continuous global coverage, in: Mission Design & Implementation of Satellite Constellations, Dordrecht, 1998, pp. 51–62. https://doi.org/10.1007/978-94-011-5088-0_5.

[9] S. Cornara, T.W. Beech, M. Belló-Mora, G. Janin, Satellite constellation mission analysis and design, Acta Astronaut. 48 (2001) 681–691. https://doi.org/10.1016/S0094-5765(01)00016-9.

[10] T. Qin, M. Macdonald, D. Qiao, Fully Decentralized Cooperative Navigation for Spacecraft Constellations, IEEE Transactions on Aerospace and Electronic Systems. Vol. 57, Issue 4, (2021) 2383–2394. https://doi.org/10.1109/TAES.2021.3060734

[11] M. Zhou, Z. Song, G. Dai, M. Wang, X. Chen, Characteristic area-based method for continuous coverage analysis of satellite constellation, IEEE Transactions on Aerospace and Electronic Systems, (2023) 1–11. https://doi.org/10.1109/TAES.2023.3287155

[12] Q.U. Hong-Song, Z. Ye, G. Jin, G., Repeat Sun synchronous orbit design method based on q value selection, Opt. Precis. Eng. 16 (2008) 1688–1694.

[13] C. Circi, E. Ortore, F. Bunkheila, C. Ulivieri, Elliptical multi-sun-synchronous orbits for mars exploration, Celest. Mech. Dyn. Astr. 114 (2012) 215–227. https://doi.org/10.1007/s10569-012-9432-0.

[14] C. Ulivieri, L. Anselmo, Multi-sun-synchronous (MSS) orbits for Earth observation, in: Proceeding of the AAS/AISS Astrodynamics Conference 123–133 (San Diego, CA, 1991).

[15] M. Aorpimai, P.L. Palmer, Repeat-groundtrack orbit acquisition and maintenance for Earth-observation satellites, J. Guid. Control Dyn. 30 (2007) 654–659. https://doi.org/10.2514/1.23413.

[16] M. Lara, R.P. Russell, Fast design of repeat ground track orbits in high-fidelity geopotentials, J. Astronaut. Sci. 56 (2008) 311–324. https://doi.org/10.1007/BF03256555.

[17] O. Abdelkhalik, A. Gad, Optimization of space orbits design for Earth orbiting missions, Acta Astronaut. 68 (2011) 1307–1317. https://doi.org/10.1016/j.actaastro.2010.09.029.

[18] S.D. Vtipil, B. Newman, Determining an Earth observation repeat ground track orbit for an optimization methodology, J. Spacecraft Rockets. 49 (2012) 157–164. https://doi.org/10.2514/1.A32038.

[19] T. Li, J. Xiang, Z. Wang, Y. Zhang, Circular revisit orbits design for responsive mission over a single target, Acta Astronaut. 127 (2016) 219–225. https://doi.org/10.1016/ j.actaastro.2016.05.037.

[20] X. He, H. Li, Analytical solutions for Earth discontinuous coverage of satellite constellation with repeating ground tracks, Chin. J. Aeronaut. 35 (2022) 275–291. https://doi.org/10.1016/j.cja.2021.11.012.

[21] F.S. Marzano, D. Cimini, A. Memmo, M. Montopoli, T. Rossi, M. De Sanctis, M. Lucente, D. Mortari, S. Di Michele, Flower constellation of millimeter-wave radiometers for tropospheric monitoring at pseudogeostationary scale, IEEE Trans. Geosci. Remote Sensing 47 (2009) 3107–3122. https://doi.org/10.1109/TGRS.2008.2012349.

[22] D. Mortari, M. De Sanctis, M. Lucente, Design of flower constellations for telecommunication services, Proc. IEEE. 99 (2011) 2008–2019. https://doi.org/10.1109/JPROC.2011.2158766.
[23] D. Mortari, M.P. Wilkins, Flower constellation set theory. Part I: Compatibility and phasing, IEEE Trans. Aerosp. Electron. Syst. 44 (2008) 953–962. https://doi.org/10.1109/TAES.2008.4655355.
[24] M.E. Avendan˜o, J.J, Davis, and D. Mortari, The 2-D lattice theory of flower constellations, Celest. Mech. Dyn. Astr. 116 (2013) 325–337. https://doi.org/10.1007/s10569-013-9493-8.
[25] J.J. Davis, M.E. Avendan˜o, and D, Mortari, The 3-D lattice theory of flower constellations, Celest. Mech. Dyn. Astr. 116 (2013) 339–356. https://doi.org/10.1007/s10569-013-9494-7.
[26] H.W. Lee, S. Shimizu, S. Yoshikawa, K. Ho, Satellite Constellation Pattern Optimization for Complex Regional Coverage, J. Spacecraft Rockets. 57 (2020) 1309–1327. https://doi.org/10.2514/1.A34657.
[27] Y. Ulybyshev, Satellite Constellation Design for Complex Coverage, J. Spacecraft Rockets. 45 (2008) 843–849. https://doi.org/10.2514/1.A34657.
[28] P. Chadalavada, D. Atri, Regional CubeSat Constellation Design to Monitor Hurricanes, IEEE Trans. Geosci. Remote Sensing 60 (2021) 1–8. https://doi.org/10.1109/TGRS.2021.3124473.
[29] W. Scott, Elements of Arithmetic and Algebra: For the Use of the Royal Military College, Royal Military College, 1 (1844) 74.
[30] S.S. Lee, C.D. Hall, Parametric approach for satellite relative orbit designs and constellations, J. Guid. Control Dyn. 44 (2021) 488–492. https://doi.org/10.2514/1.G005440.
[31] P.Y. Tuyetdong, G. Elysus, Hypocycloids and Hypotrochoids, MathAMATYC Educator, Vol. 6, No. 1, (2014)
[32] D. Arnas, D. Casanova, E. Tresaco, Time distributions in satellite constellation design, Celest. Mech. Dyn. Astr. 128 (2017) 197–219. https://doi.org/10.1007/s10569-016-9747-3.

Vitae

Soung Sub Lee is an associate professor at Sejong University in ROK. He graduated from ROK Air Force Academy and received a master's degree from Yonsei University. In 2009, he received a Ph.D. in space engineering from Virginia Tech. His research interests are in the field of dynamics and control of satellite relative motions. Recent research has focused on the extension and development of the newly proposed Satellite Constellations theory.